Reconstructing meteoroid trajectories using forward scatter radio observations from the BRAMS network

Joachim Balis[1,2], Hervé Lamy[1], Michel Anciaux[1], Emmanuel Jehin[2]

[1] **Royal Belgian Institute for Space Aeronomy**
Brussels, Belgium
joachim.balis@aeronomie.be herve.lamy@aeronomie.be michel.anciaux@aeronomie.be

[2] **STAR Institute, University of Liège**
Liège, Belgium
ejehin@uliege.be

This paper summarizes the recent improvements made in retrieving meteoroid trajectories using data from the forward scatter radio system BRAMS. Two methods are presented, one based only on the knowledge of time delays measured between meteor echoes observed at the receivers, and one including information from a radio interferometer in addition to the time delays measurements. For comparison about the quality of trajectory reconstruction, data from the optical CAMS-BeNeLux network are used. This work contains results available in September 2022, built on previous results from (Lamy et al. 2021). Discussions about current developments and future improvements are provided at the end of the paper.

1 Introduction

The BRAMS (Belgian RAdio Meteor Stations) network is a Belgian project using forward scatter of radio waves to detect and characterize meteoroids. It comprises a dedicated transmitter located in the South-West of Belgium and 44 receiving stations spread all over the Belgian territory and neighbouring countries (see Figure 1 for status in September 2022)

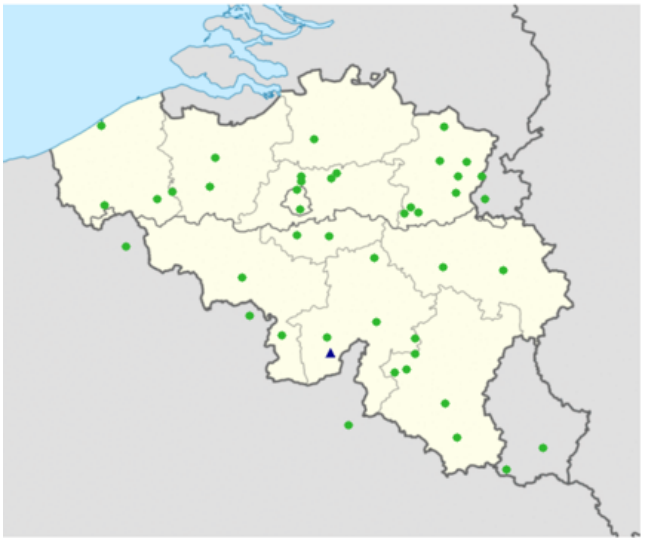

Figure 1 – Map of the BRAMS network in September 2022. The blue triangle is the transmitter located in Dourbes while the green dots are the 44 active receiving stations at the time.

The transmitter emits a circularly polarized continuous radio wave with no modulation at a frequency of 49.97 MHz with a power of 130 Watts. All the receiving stations are using a 3-element Yagi antenna set-up vertically and oriented in azimuth on the transmitter. At the time of writing, approximately a third of the receiving stations are using analog ICOM-R75 receivers, an external sound card to sample the signal coming from the antenna, and are controlled by the freeware program Spectrum Lab running on a PC (see e.g. Lamy et al. 2015). The other half uses digital SDR-RSP2 receivers controlled by a Linux system running on a Raspberry Pi (Anciaux et al. 2020). All stations are equipped with a Garmin GPS that provides timestamps to the BRAMS data and allows a time synchronization between the receiving stations. Additional features of the receiving stations are not described here. Instead, we refer the reader to previous publications in the Proceedings of the IMC (Lamy et al. 2015, Anciaux et al. 2020).

One of the difficulty with forward scatter systems is the determination of individual meteoroid trajectory and speed as the geometry is more complex than in the case of backscatter systems. In the specific case of BRAMS, the absence of modulation in the CW transmitted signal does not allow to estimate the total range traveled by the radio wave between the transmitter (Tx), the reflection point and the receiver (Rx), and therefore makes the problem very complex. We present here an approach to retrieve meteoroid trajectories using BRAMS data. This approach has been improved and extended compared to the results presented in (Lamy et al., 2021). Two methods are considered: one based only on measurements of time delays between meteor echoes recorded at different receiving stations, and one using the same data but complemented with data from the radio interferometer located in the Humain station which provides the direction of one specular reflection point. In order to assess the quality of the reconstruction, a comparison with data from the CAMS-BeNeLux network is provided.

2 Two methods to determine meteoroid trajectory and speed

The first method (hereafter called Method 1) is based purely on geometrical considerations and relies on the specularity condition of the reflection of the radio wave. The specular reflection point is the point along the meteoroid path for which the total distance traveled by the radio wave is minimum, which means that the total distance $S_i = R_{Ti} + R_{Ri}$ (where R_{Ti} is the distance from the transmitter to the meteor and R_{Ri} is the distance meteor-receiver) must be minimum for each receiving station i. Because the geometry Tx-$\mathrm{Rx_i}$ is different for each receiving station $\mathrm{Rx_i}$, the corresponding reflection points will be located at various positions along the meteoroid path. This is illustrated in Figure 2 for a reference station $\mathrm{Rx_0}$ and another station Rx_i. In this example, the specular reflection point P_0 for the reference station is created before the corresponding reflection point P_i. The distance between the two points depends on the speed of the meteoroid which is here assumed constant. As a consequence, the reference station will detect a meteor echo shortly before receiving station i, the time delay between meteor echoes depending on the meteoroid path and speed.

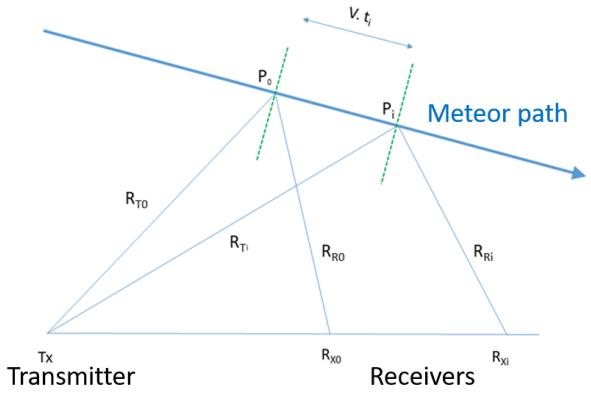

Figure 2 – Specularity and geometry of a forward scatter set-up.

A meteoroid trajectory can be defined by the 3D Cartesian coordinates of one specular point (the one corresponding to a reference station) and the three components of the velocity which provides the direction (assuming again a constant speed). This gives a total of six unknowns (respectively called X_0, Y_0, Z_0, v_x, v_y and v_z) and therefore the need to have at least six equations to avoid solving an underdetermined system. In Method 1, these equations are provided by the fact that the total derivative, dS_i/dt, must be equal to 0 for at least six stations $i = 1, \ldots, 6$. This leads to a set of ≥ 6 non-linear equations which contains the 6 unknowns and the time delays Δt_i between meteor echoes recorded at station i and the reference station. A non-linear solver must then be used to solve this set of equations and taking into account additional constraints on the unknowns, such as the height of all reflection points which must lie between e.g. 80 and 120 km altitude, or the speed of the meteoroid which must be larger than $\sim 11\,\mathrm{km/s}$ but smaller than $\sim 72\,\mathrm{km/s}$.

As discussed for the CMOR network in (Mazur et al., 2020), this inverse trajectory reconstruction problem is severely ill-conditioned when all the receiving stations lie close to the same plane. This is the case here since the differences in altitude between the receivers are only of a few tens of meters while the trajectories are located at about 100 km in altitude. In this configuration, the output trajectory will be highly sensitive to the quality of the input time delays, small errors on the latter leading to large uncertainties on the output trajectory.

The second method (hereafter called Method 2) is using the same assumptions as Method 1 but includes data from our interferometric radio station located in Humain. Unlike the other receiving stations, it uses 5 antennas in the so-called Jones configuration (Jones et al. 1998, Lamy et al. 2017) and allows to determine the direction of arrival of the meteor echo to within approximately 1°. The interferometer provides two more equations for the azimuth and elevation of the specular reflection point but does not provide its exact position. With these additional equations, we only need time delays measured between 3 additional stations and a reference station in order to get at least 6 equations. This interferometric information appeared to alleviate the ill-conditioning of the trajectory reconstruction problem.

3 Solver validation

To validate the trajectory reconstruction solver, 11 simulated trajectories are studied. They are inspired from optical data given by the CAMS BeNeLux network (Jenniskens et al., 2011 ; Roggemans et al., 2016). Data were provided for 2 clear consecutive nights from 29 to 31 July 2020, in a period without any strong activity from meteor showers. Among the 948 available trajectories, a selection was made based on the following criteria : (i) most of the trajectories are not located above Belgium and therefore not geometrically suitable to be detected by our BRAMS receiving stations, (ii) each trajectory must be detected by at least 6 stations, otherwise we reject it, (iii) because we want to compare Methods 1 & 2, one of these stations must be the interferometer in Humain, and (iv) we restrict ourselves as much as possible to underdense meteor echoes in order to ensure that the specularity condition is valid. The application of these criteria resulted in a selection of 12 suitable CAMS trajectories. The parameters of these trajectories are summarized in Table 1.

The idea behind those simulated trajectories is to verify the proper functioning of the solver when there are no measurement errors, i.e. checking that we recover the targeted trajectory assuming we have a perfect knowledge of the time delays at the receivers. To do so, the trajectory is used to get the theoretical time delays. The latter are then fed inside the trajectory reconstruction solver.

N°	X_{Hum} (km)	Y_{Hum} (km)	Z_{Hum} (km)	V_x (km/s)	V_y (km/s)	V_z (km/s)	V_{norm} (km/s)	El. [°]
79	44.32	59.12	94.90	−24.07	30.56	−12.43	40.84	17.72
105	121.59	95.17	99.39	−18.41	33.58	−12.56	40.30	18.16
149	−88.81	94.47	88.37	5.1	19.96	−13.89	24.85	33.98
188	−52.88	−23.11	88.13	0.54	28.29	−5.52	28.83	11.04
282	−96.09	35.92	88.28	−2.81	36.22	−16.61	39.95	24.58
477	−77.35	11.33	104.9	−34.5	−38.65	−29.93	59.84	30.01
532	38.66	51.65	91.67	−25.86	30.63	−11.60	41.73	16.14
536	21.61	199.76	105.64	−58.08	13.41	−26.15	65.09	23.69
598	6.17	158.68	103.13	−70.94	−4.66	−5.34	71.30	4.29
709	−32.21	108.29	97.79	−37.38	22.92	−45.33	63.07	45.96
773	−92.9	61.6	98.19	−36.29	13.66	−50.26	63.48	52.35

Table 1 – CAMS trajectories for the solver validation. X_{Hum}, Y_{Hum}, and Z_{Hum} are the coordinates of the specular reflection point for the Humain station in a Cartesian referential centered on the Dourbes transmitter. X is directed East-West and counted positive towards East, Y is directed North-South and counted positive towards North. V is the (constant) speed of the meteoroid. El. is the complement of the zenith angle described by the trajectory.

Several inverse MATLAB solvers were tested and they all yielded errors of the same order of magnitude on the 11 reconstructed trajectories: about 0.001° on the inclination angle, a few meters on the reflection point location and about 1 m/s on the velocity. This analysis demonstrates the proper functioning of our solver as it yields the correct solution if the inputs are perfectly known.

In practice, the input time delays are obtained through a post-processing procedure described in the following section. The corresponding uncertainties on the timings determination will lead to uncertainties on the output trajectories, as discussed in Section 2.

4 Determination of time delays

The start of the meteor echo is chosen as the time when it rises to approximately 50 % of its peak amplitude. This should indeed correspond to the instant at which the specular reflection occurs.

Meteor echoes are first identified in the BRAMS spectrograms based on their approximate expected time of appearances which correspond to the passage of the meteoroid at the reflection points. These times are computed based on the initial time and height of the CAMS trajectory, and on the speed of the meteoroid. A visual inspection was done for this study to avoid selecting another meteor echo randomly appearing at approximately the same time. An automatic procedure is planned for this task in the future. Once the meteor echoes have been identified in the spectrograms, their frequency range can be computed automatically (see top panel of Figure 3). If this frequency range contains the frequency of the direct signal coming from the transmitter, the latter is first reconstructed using a local FFT and then subtracted from the raw data (see middle panel of Figure 3). A Blackman filter of high order is then used to remove the noise at frequencies where the meteor echo does not appear. After these two steps, an accurate determination of the start of the meteor echo can be computed on the amplitude profile (see bottom panel of Figure 3).

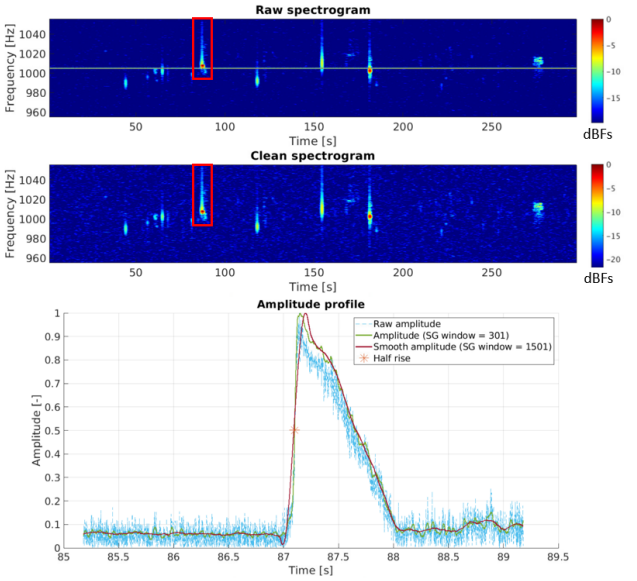

Figure 3 – Top panel: Example of a spectrogram and a meteor echo detected in the spectrogram of Humain (red rectangle). Middle panel: Same spectrogram obtained after subtracting the reconstructed direct signal coming from the transmitter from the raw data. Bottom panel: Amplitude profile (in blue) of the meteor echo obtained after bandpass filtering. 2 curves with different Savitky-Golay smoothings are shown.

5 Results with both methods

The MATLAB solver used to resolve the set of non-linear equations described in section 2 is *fmincon* which searches for the set of unknowns that minimizes the sum of the squares of the difference between the measured time delays and the modeled ones.

Method 1 using only time delays is shown on Figure 4 for trajectory 79. This figure presents the projected CAMS trajectory as well as the reconstructed one in the horizontal XY plane and in a 3D frame, where coordinates X,Y, and Z are given in a local Cartesian frame

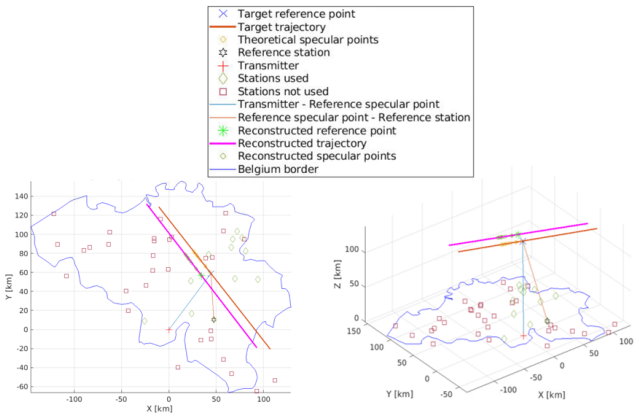

Figure 4 – Example of result obtained for CAMS trajectory 79 using Method 1.

centered on Dourbes. Despite that the location of Humain specular point is off by about 17 km, the velocity is accurate within 5 % compared to the CAMS data (40.2 instead of 41.7 km/s), and the inclination is off by less than 0.7°.

Figure 5 presents the results obtained for trajectory 79 in the same horizontal and vertical planes but using Method 2. Since the direction of the reflection point is constrained via equations including the interferometer data, it is now correctly retrieved and this helps greatly the reconstruction of the trajectory. The altitude of the reflection point becomes much more accurate with an error of less than 0.7 km. The speed direction is accurate to 0.2° and the velocity (41.3 km/s) is very close to the one measured by CAMS.

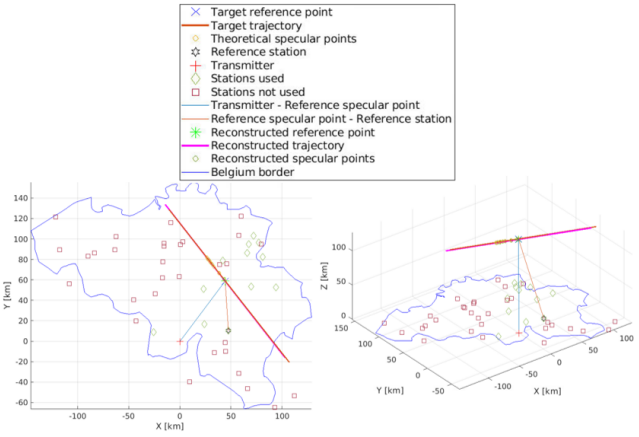

Figure 5 – Example of result obtained for CAMS trajectory 79 using Method 2.

6 Discussions and perspectives

Method 1 is very important since it is the only one that can be applied to all archived BRAMS data of the last 10 years. It is unfortunately extremely ill-conditioned (i.e. very sensitive to the quality of the inputs). However, thanks to the various improvements and corrections brought since IMC 2021, it works on several cases and gives good agreement with optical data in terms of inclination and velocity. Still, it does not work on every trajectory and gives large errors in terms of specular point location. In that respect, Method 2 works much better, but unfortunately cannot be applied to a lot of data since it requests to have at least 3 stations detecting the same meteor as the interferometer located in Humain. As a result, one priority in the near future will be to build another interferometer in the north of Belgium.

Given the current limitations of Method 1, we are currently extending the pre-t0 phase approach described for backscatter radars in (Mazur et al., 2020). This approach uses the phase of the signal before the specular point in order to get back the velocity of the meteoroid. It provides two important benefits. On the one hand, it further constrains the trajectory solver by adding extra inputs, thus reducing the sensitivity of the output trajectory on the input time delays. On the other hand, it allows to get some insight on the deceleration of the meteoroid during its upper atmosphere travel, which cannot be done with the approach described in this paper as we assumed a constant speed motion.

7 Acknowledgement

The BRAMS network is funded partly by the Solar-Terrestrial Center of Excellence (STCE). The BRAMS project is an active Pro-Am collaboration. We would like to thank all operators hosting the receiving stations.

8 Reference details

1. Lamy H., Balis J., Anciaux M. (2021). Reconstructing meteoroid trajectories using BRAMS data. WGN, the Journal of the IMO, 49:6, 195-200.

2. Anciaux M.; Lamy H. ; Martinez Picar A. ; Ranvier S. ; Calders S. ; Calegaro A.; and Verbeeck C., The BRAMS receiving station v2.0, Proceedings of the International Meteor Conference, Bollmannsruh, Germany, 03-06 October 2019 Eds.: Pajer, U.; Rendtel, J.; Gyssens, M.; Verbeeck, C. International Meteor Organization, ISBN 978-2-87355-033-2, 39-42, 2020

3. Jenniskens P. ; Gural P. ; Grigsby B. J. ; Newman K. E. ; Borden M. ; Koop M. ; Holman D., CAMS : Cameras for allsky meteor surveillance to establish minor meteor showers. Icarus, 216 :40-61, 2011, doi: 10.1016/j.icarus.2011.08.012

4. Jones J. ; Webster R. ; Hocking W., An improved interferometer design for use with meteor radar. Radio Science, 33, 55-65, 1998, doi: 10.1029/97RS03050

5. Lamy H. ; Anciaux M. ; Ranvier S. ; Calders S. ; Gamby E. ; Martinez Picar A. ; Verbeeck, C. ; Recent advances in the BRAMS network, Proceedings of the International Meteor Conference, Mistelbach, Austria, 27-30 August 2015, Eds.: Rault, J.-L.; Roggemans, P., International Meteor Organization, ISBN 978-2-87355-029-5, 171-175, 2015

6. Lamy H. ; Tétard C., Retrieving meteoroids trajectories using BRAMS data : preliminary simulations, Proceedings of the International Meteor Conference, Egmond, the Netherlands, 2-5 June 2016, Eds.: Roggemans, A.; Roggemans, P., ISBN 978-2-87355-030-1, 143-147

7. Lamy H. ; Tétard C. ; Anciaux M. ; Ranvier S. ; Martinez Picar A. ; Calders S. ; Verbeeck, C., First observations with the BRAMS radio interferometer, Proceedings of the International Meteor Conference, Petnica, Serbia, 21-24 September, 2017 Eds.: Gyssens, M.; Rault, J.-L. International Meteor Organization, ISBN 978-2-87355-031-6, 132-137

8. Mazur M. ; Pokorny P. ; Brown P. ;Weryk R. ; Vida D. ; Schult C. ; Stober G. ; Agrawal A., Precision measurements of radar transverse scattering speeds from meteor phase characteristics. Radio science, 55, 1-32, 2020, doi: 10.1029/2019RS006987.

9. Roggemans P., Johannink C., and Breukers M. (2016). Status of the CAMS-BeNeLux network". In Roggemans A. and Roggemans P., editors, Proceedings of the International Meteor Conference, Egmond, the Netherlands, 2-5 June 2016. IMO, 254-260.